Chapter 3

Recrystallization of Rolled α-Zr Single Crystals

Yu Perlovich and M. Isaenkova

Additional information is available at the end of the chapter

http://dx.doi.org/10.5772/60019

1. Introduction

Recrystallization of metal material is a complicated phenomenon that unites different aspects of its profile, including plastic deformation, strain hardening and behaviour by heat treatment. The latter entails numerous processes such as recovery, growth of recrystallization nuclei and the competition of new grains. When considering the plastic deformation of single crystals, the experimental analysis of their ensuing recrystallization becomes simpler: in the grains of a polycrystal, plastic deformation creates a wide spectrum of substructures depending on the crystallographic orientation of grains, whereas in the case of a deformed single crystal, initial substructure conditions are much more limited.

In principle, concepts of 'polycrystal' and 'single crystal' ought to be associated with the concept of that of 'deformed single crystal'. The single crystal, subjected to plastic deformation (most often one deals with rolled single crystals) does not become a polycrystal; at the same time, it ceases to be a single crystal, because of the crystallographic texture that forms in it due to the number of initial orientations of this single crystal. A rolled polycrystal is a conglomerate of rolled single crystals, but a rolled single crystal differs from a polycrystal (or a rolled polycrystal) in terms of boundary characteristics, which separate regions with different orientations. In the polycrystal, these regions correspond to individual grains and are separated from neighbours by high-angular boundaries. In the rolled single crystal, these regions originate from the same monocrystalline matrix, due to the inevitable non-uniformity of plastic deformation; therefore, they are separated from neighbours by low-angular boundaries, except for the case of twinning, which was most often observed in the current work.

Experiments involving the rolling of single crystals can provide results that may be unreachable by similar experiments with polycrystals. Among such results is the obtaining of quasi-monocrystalline foils by the cold rolling of BCC single crystals (Mo, Nb) in the case of initial orientation {001}<011>. These foils are characterized by minimal strain hardening up to the

highest deformation degrees and do not recrystallize by subsequent annealing [1]. At the same time, rolled single crystals with other initial orientations acquire significant strain hardening and can even be destroyed under rolling. These effects make clear the mechanisms of plastic deformation and recrystallization of materials, and indicate how the substructure of polycrystalline products can be modified and optimized. To date, the existence of analogous effects in the rolling of α-Zr single crystals have not been investigated due to difficulties related to procuring them.

Though the title of this chapter is "Recrystallization of rolled α-Zr single crystals", the intention of authors is wider and concerns also recrystallization of rolled polycrystalline α-Zr, since the behaviour under annealing of rolled single crystals helps to explain some known features of recrystallization in polycrystals and can compare the characteristics of strain hardening distribution in rolled single crystals and polycrystals.

2. Reorientation of grains and texture development in α-Zr under rolling

When considering recrystallization and especially its textures, it is necessary to take into account the prehistory of the material, including features of its previous deformation, grain reorientations, formed deformation textures and plastic deformation mechanisms. Therefore analysis of recrystallization inevitably expands in scope and covers a number of adjacent questions, among them, the details concerning preceding grain reorientation. Thus, in the current chapter, recrystallization is considered as a derivative effect of plastic deformation.

As a preamble to discussing the behaviour of α-Zr single crystals under rolling, we take into account the Hobson's calculated diagram for operating plastic deformation mechanisms [2] and our X-ray experimental observations of basal axes (or axis) trajectories during the course of rolling [3, 4]. The Hobson's diagram, added later by Matcegorin et al. [5] (Fig. 1), predicts slip and twinning systems operating in α-Zr grains in conditions of cold rolling. Three twinning systems are considered: (1) $\{10\bar{1}2\}\langle\bar{1}011\rangle$ and (2) $\{11\bar{2}1\}\langle\bar{1}\bar{1}26\rangle$, activated by the tension between angles of basal axes (or axis) reorientations at 85° and 35°, respectively; (3) $\{11\bar{2}2\}\langle\bar{1}\bar{1}23\rangle$, activated by compression and with a 64° angle of reorientation. In [2] and [5], for polycrystalline Zr-based alloy regions, the stereographic projections are drawn under which rolling prismatic, basal and pyramidal slip systems operate. Experimental trajectories of basal axes in cold-rolled α-Zr grains [3, 4, 6] contain jump-like segments with an angular length of 10-15°, which testify in particular to possible twinning by corresponding systems (Fig. 2-3). The unique evidence of twinning in the annealed polycrystalline plate of the Zr-1%Nb alloy consists in the sharp jump-like reorientation of basal axes in the surface layer of a plate at the first moment of its tensile deformation along a transverse direction. Due to twinning basal axes change their orientations in the jump-like manner and get from vicinity of pole figure diameter ND-TD to regions near its diameter ND-RD [4].

Additionally, it was found [6] that development of the rolling texture in polycrystalline α-Zr has three stages:

1. formation of the quasi-stable texture T1 (0001)±15-20°ND-RD $\langle 11\bar{2}L\rangle$

http://dx.doi.org/10.5772/60019

2. transition T1 → T2,

3. perfection of the stable texture T2 (0001)±30-40°ND-TD <10$\bar{1}$0>.

Texture T1 is supported due to an equilibrated slip at the basal and pyramidal planes, transition T1 → T2 is connected with the strain hardening of pyramidal slip systems and the stability of the final rolling texture T2 is conditioned by an equilibrated slip through basal and prismatic planes (Fig. 4). The jump-like reorientation of basal axes due to twinning by planes {11$\bar{2}$1}, revealed experimentally, throws them into the neighbouring region of the basal slip shown in the diagram in Fig. 1 [4], thereby moving basal axes further to the centre of stereographic projection. The continuous arrows coinciding with experimentally observed reorientation trajectories through the slip of basal axes (Fig. 4) are finally directed to the maxima of rolling textures T1 or T2. This indicates that in polycrystalline α-Zr, the rolling texture develops mainly by means of basal, pyramidal and prismatic slip.

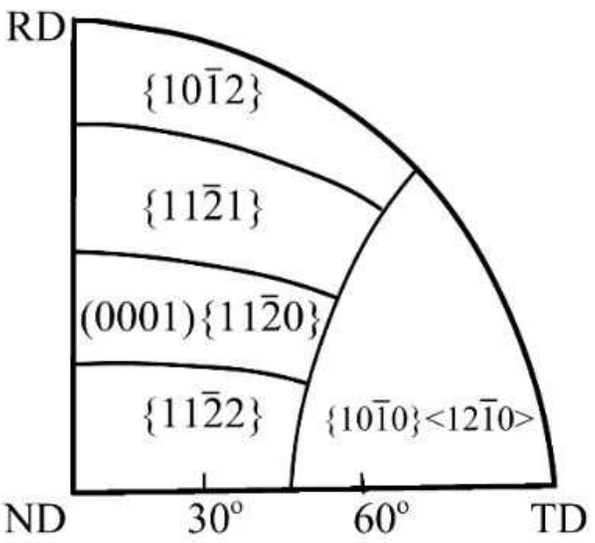

Figure 1. Regions of stereographic projection for the α-Zr sample, whereby its rolling, different deformation systems operate depending on the orientation of the grain basal axis. Calculated systems are characterized by the largest values of the Schmidt factor. Assumptions were made that each system has the same critical stress and that $\sigma_{RD} = \sigma_{TD}$[5].

Development of the rolling texture in α-Zr single crystals was studied as applied to coarse-grained samples [7], since lattice reorientation in separate coarse grains as a first approximation occurs independently of similar processes in other grains. However, the formation of the recrystallization texture in the same coarse-grained sample includes the growth of nuclei at grain boundaries, resulting in this process moving outside of separate grains and its control via the orientations of neighbouring grains. Therefore, recrystallization in rolled coarse-grained samples does not imitate the situation in rolled single crystals. Thus, the current study is the first X-ray investigation of recrystallization in cold-rolled α-Zr single crystals.

As for recrystallization of cold-rolled polycrystalline α-Zr, its regularities were described in detail in [8-9]: reorientation of prismatic axes by 30° about the basal axis, the shift of basal axes along the TD-ND diameter of stereographic projection in the direction of ND and in the case of multicomponent rolling, texture redistribution of its components according to definite relationships. However, these data were obtained only by the geometric analysis of texture features, without the use of data concerning the distribution of strain hardening in rolled polycrystals. Therefore, the motive power of recrystallization in the considered concrete cases is unclear. Currently, the X-ray method of generalized pole figures is being developed [10, 11], which allows revealing the distribution of strain hardening in textured materials, depending on the crystallographic orientation of their grains. This will allow a better understanding of the reasons for the observed passage of recrystallization.

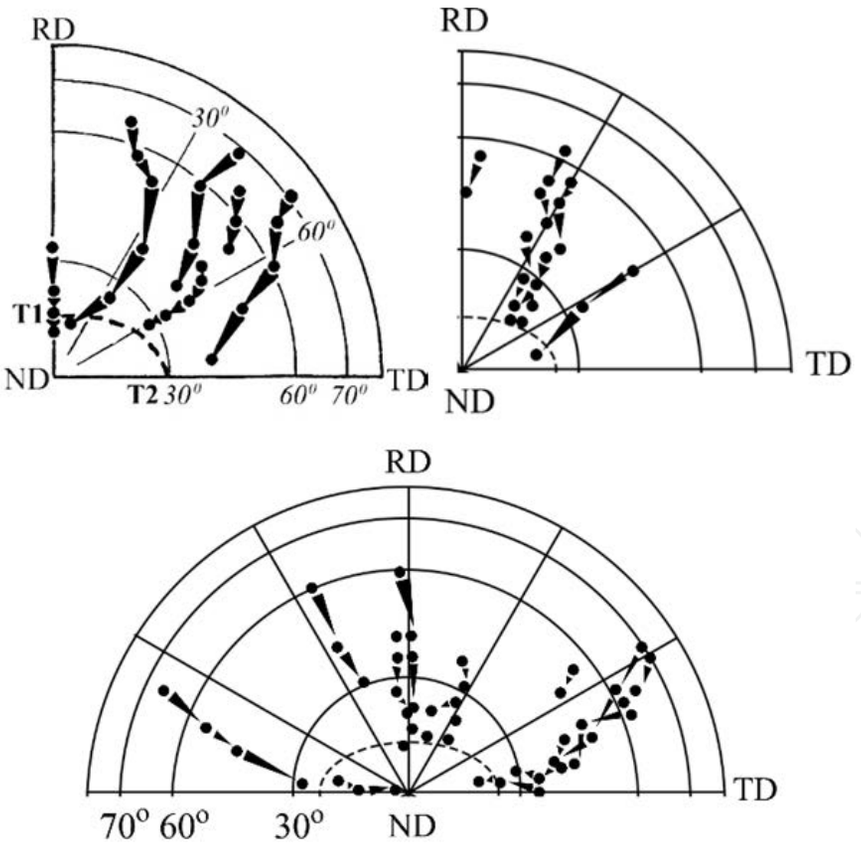

Figure 2. Examples of the experimental trajectories of basal axes reorientations during the course of cold rolling of Zr and its alloys.

http://dx.doi.org/10.5772/60019

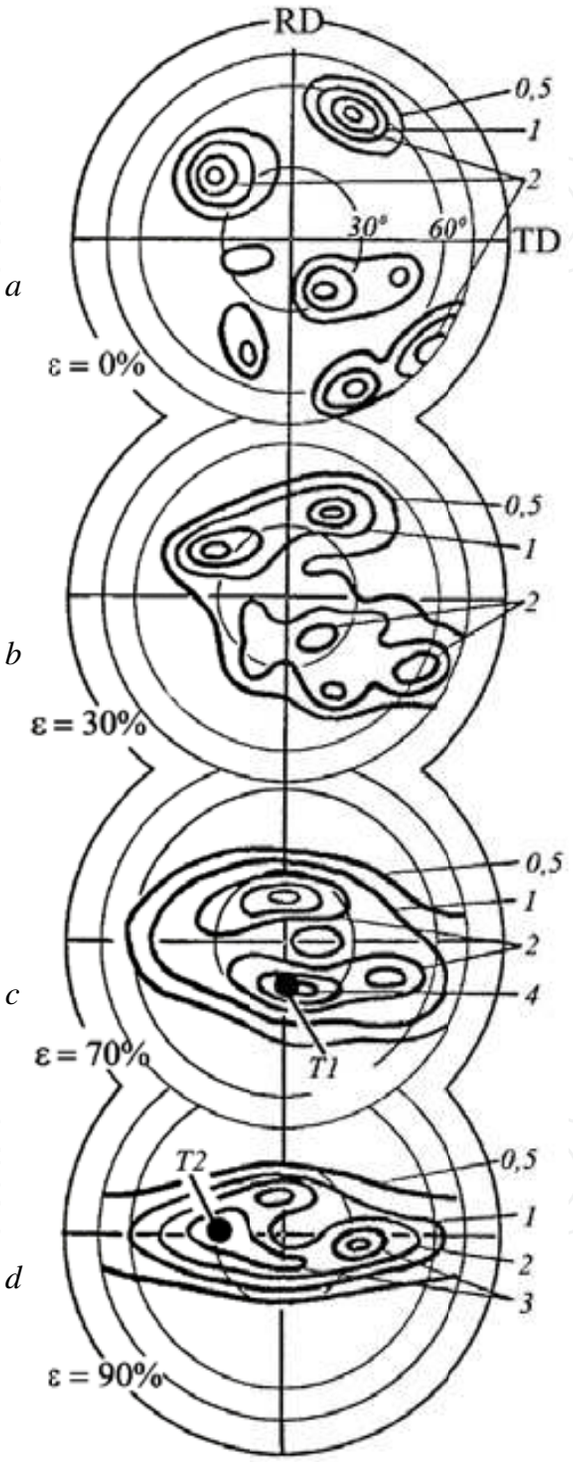

Figure 3. Evolution of PF (0001) for α-Zr by increasing the deformation degree through cold rolling.

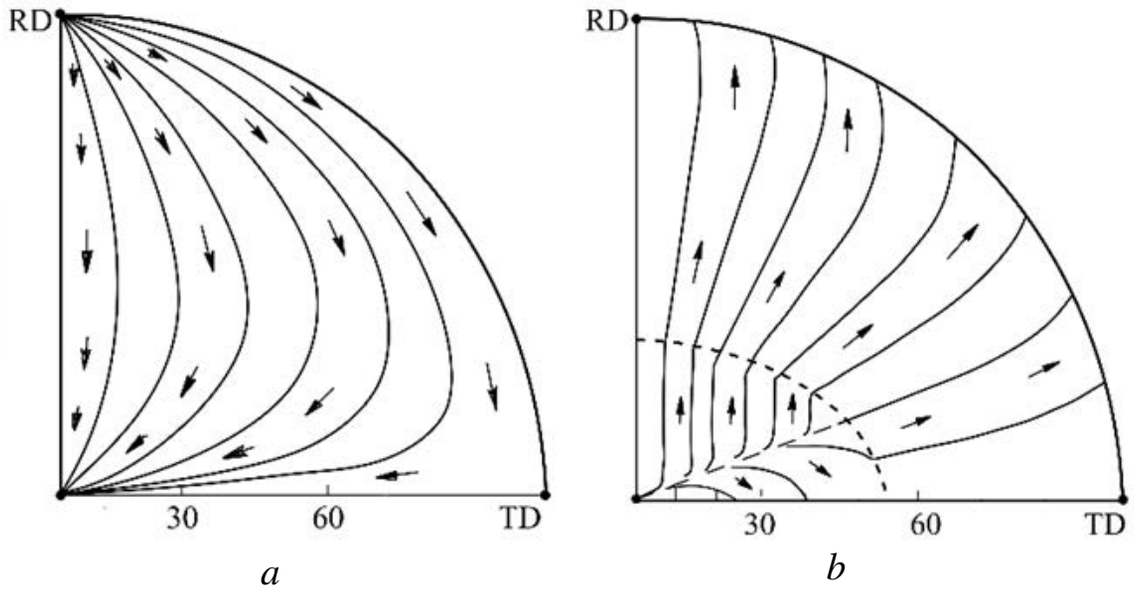

Figure 4. Calculated trajectories of basal axes reorientations during the course of rolling through the operation of basal (a) and pyramidal (b) slip systems [5].

3. Experimental procedure: Studied samples and used X-ray methods

A single crystal of pure Zr was obtained by means of solid-phase over-crystallization. Samples 7x10x3 mm in size were cut from the cylindrical single crystal using the electro-erosion method. Obtained samples were rolled at a laboratory rolling mill between plates of stainless steel up to the deformation degree ε_{max}= 80% and with ~5% reductions per pass.

The initial monocrystalline plate and rolled single crystals were subjected to X-ray texture investigation, which included (1) texture analysis using the method of direct pole figures; (2) the study of the strain hardening distribution using the method of generalized pole figures (GPF) (see the next section).

Then, rolled single crystals were annealed in the evacuated vessel at 580°C for 3 h, the standard regime of recrystallization heat treatment for industrial products made from Zr-based alloys. After annealing, rolled single crystals were repeatedly subjected to X-ray investigation; direct pole figures were measured once more and subtraction diagrams were constructed on the basis of texture data treatment (see the next section).

In addition to the investigation of rolled α-Zr single crystals, the current work also included the study of cold-rolled and recrystallized (1) coarse-grained iodide Zr and (2) a polycrystalline sheet of Zr-1%Nb alloy, rolled along RD and along TD. The development of rolling textures, distributions of strain hardening and recrystallization textures in these samples was studied using the same X-ray methods as those used in the study of rolled single crystals. When comparing X-ray data obtained for rolled single crystals and polycrystalline samples, a number

http://dx.doi.org/10.5772/60019

of important conclusions concerning the regularities of their strain hardening and recrystallization were made.

All X-ray studies of the used samples were carried out using an X-ray diffractometer Bruker D8 DISCOVER with a LynxEye position-sensitive detector. Partial direct pole figures PF(0001) and $\{11\bar{2}0\}$ were constructed with an angular radius 80° [12].

3.1. The method of Generalized Pole Figures (GPF)

For rolled α-Zr single crystals, the X-ray method of generalized pole figures (GPF) was used. This method consists of registration of X-ray line profiles during the course of texture measurement [10, 11]. In the current case, the method characterized the condition of the crystalline lattice along basal axes <0001> in all grains of the sample. The physical angular half-width β_{0002} of the X-ray line (0002), increasing as a result of strain hardening and decreasing by recrystallization was used as a measure of crystalline lattice distortion. A wide spectrum of substructure conditions, i.e., values of β_{0002}, the distribution of which in the stereographic projection is shown with GPF β_{0002}, corresponded to separate micro-fragments of the rolled single crystal or grains of rolled polycrystal, and the optimal criterion for systematization of GPF data was their crystallographic orientation.

In particular, for many rolled metal materials with the developed texture it was revealed that the strain hardening of fragments (grains, subgrains, crystallites) corresponding to texture maxima was significantly lower than that for texture minima. Strain hardening increased as grain orientation shifted from a texture maximum to a texture minimum. In cold-rolled BCC metals, where primary recrystallization is realized by the growth of grains with increased strain hardening, new maxima of the recrystallization texture grew at the maxima "slopes" of the rolling texture. Hence, strain hardening of these grains was sufficiently high for their predominant growth; at the same time, there were a sufficient amount of grains with such orientation for them to be able to "swallow" the rest of the deformed matrix.

Application of the GPF method requires the availability of an X-ray texture diffractometer of last models with a position sensitive detector, which will allow registering the entire X-ray line profile by texture measurement, without time losses for movement of the detector. The procedure of GPF measurement and construction requires special software, which can be developed on the basis of the standard technical potential of BRUKER diffractometers.

3.2. The method of mutual subtraction of texture Pole Figures (PF)

In order to reveal regions of pole density changes in PF(0001) through the transition from cold-rolled to recrystallized α-Zr, difference diagrams $S(\psi,\varphi)$ are constructed in which (ψ,φ) are the angular coordinates of points in PF and $S(\psi, \varphi)$ is equal to the difference between pole densities in corresponding points of PF(0001) for recrystallized and cold-rolled samples; thus, $S(\psi, \varphi) = [PF(0001)_{recr}\text{-}PF(0001)_{roll}]$. Inhomogeneous strain hardening and recovery result in some violation of proportionality between scattering ability, calculated pole density and specific volumes of deformed and recrystallized grains. In this connection, pole densities in the PF of rolled and recrystallized samples can be compared only with limited accuracy. Therefore,

subtraction diagrams are constructed only for those regions of $PF(0001)_{roll}$ where pole densities noticeably exceed the sensitivity of texture measurements. In the current case, this threshold value of pole density was accepted as 0.5. Represented below, subtraction diagrams visually demonstrate the arrangement of regions with maximal changes of pole density as a result of recrystallization.

4. Experimental results

4.1. Twinning as the main deformation mechanism of α-Zr single crystals

In Fig. 5a, the partial direct PF{11$\bar{2}$0} with an angular radius of 80° is presented for the initial α-Zr single crystal. The axis of the initial cylindrical single crystal is situated in the centre of PF; it coincides with the normal direction of the plate cut from the crystal and is perpendicular to the direction of its following rolling. In the same PF, near the circumference of stereographic projection with an angular radius of 80° the exit of the basal axis [0001] is shown. This is represented by concentric circular contours and is distanced by an angle of 90° from the exits of prismatic axes <11$\bar{2}$0>. After rolling of the single crystal up to a deformation degree of ~5%, essential changes take place in its stereographic projection: jumping from the PF(0001) shown in Fig. 5b, due to the activation of twinning by planes {11$\bar{2}$1}, the basal axis reorients by ~35°, whereas due to twinning by plains {10$\bar{1}$2} reorientation occurs by ~85°. When rolling the single crystal by 53%, the texture maximum formed by twinning strengthens due to further twinning in regions of the single crystal with the initial orientation and additionally shifts by ~15°-20° due to basal slip [5] (Fig. 5-*c*). The ensuing rolling of up to ε=80% leads to formation in the rolled single crystal of a two-component texture (Fig. 5d) typical for α-Zr [6, 13].

The same cycle of investigations was repeated for monocrystalline plates of three initial orientations, differing only in terms of RD. These orientations corresponded to the following angular coordinates of basal axes: N 1 - (70°, 33°); N 2 - (70°, 152°); N 3 - (70°, 87°). The three columns of PFs in Fig. 5 demonstrate the successive stages of rolling texture development in single crystals within the following indicated orientations: N 1 - (*a-d*), N 2 - (*e-i*), N 3 - (*j-n*). The first stages of all three successions in Fig. 5 corresponded to the deformation degree ε≈5-7% in order to create mutually differing distributions of monocrystalline fragments resulting from various positions of twinning systems relative to the RD. By considering the obtained data it became evident that twinning was the main plastic deformation mechanism of α-Zr single crystals.

After deformation by only 5-7%, the texture maximum in PF(0001) characterizing the initial orientation of a single crystal broke into five-six new maxima corresponding to the reorientation of single crystal fragments by means of twinning in planes {10$\bar{1}$2}, {10$\bar{1}$1} and {11$\bar{2}$1} (Fig. 5b, e, j). The initial orientation of prismatic axes of the single crystal (Fig. 5a) and the characteristic reorientation angles of basal axes at 85°, 57° or 123° and 35°, shown in Fig. 5b, e, j, allowed for identifying unique operating systems of twinning. The primary planes of twinning in these cases were {10$\bar{1}$2} and {11$\bar{2}$1}, resulting in the formation

of texture maxima, which are indicated by red and blue arrows, respectively (see Fig. 5-b, e, j). Consequently, maxima situated near ND had the greatest intensity. Additional weak texture maxima, marked by Figures 1-4 in Fig. 5e and j, formed due to twinning of the initial single crystal by planes $\{10\bar{1}1\}$ (green arrows in Fig. 5e). These maxima proved to be unstable due to their orientation (Fig. 5f) and disappeared at subsequent stages of rolling, providing texture scattering (Fig. 5g). Twinning by planes $\{10\bar{1}1\}$ had previously not been considered in the analysis of rolling texture formation in α-Zr [2, 5-7].

The above-described changes of basal axes orientations when rolling α-Zr single crystals with orientations N 1 and N 2 agreed with the proposed diagram by Hobson of plastic deformation mechanisms activated in α-Zr grains with different orientations of basal axes relative to external directions ND, RD and TD [2, 5]. The process of twinning continues until where some regions with the initial orientation remain in the single crystal.

This process is described using curves that show changes in PF parameters as the deformation degree increases (Fig. 6). Among these parameters, there are angular positions ψ and intensities P of initial texture maxima *A* and new texture maxima *B*, formed by twinning. Solid lines in Fig. 6 show changes in position and intensity of initial maxima *A*, whereas dotted lines indicate changes of position and intensity of derived maxima *B* for rolled single crystals N 2 (*a, b*) and N 3 (*c, d*). In particular, one can see that in both single crystals, derivative maxima *B* arose at deformation degrees 3-5%, whereas maximum *A* in PF(0001) for the single crystal N 2 disappeared by 13% after rolling. The decrease in P intensity for all maxima indicates the further fragmentation of the single crystal by means of twinning, including regions corresponding to both *A* and *B* maxima. The shift of maximum *A* in PF(0001) for the single crystal N 3 was connected with operation of the slip. In this single crystal, the basal axis of which was oriented near TD, twinning by planes $\{10\bar{1}2\}$ also activated.

At the next stages of deformation in the single crystal N 2, twinning by planes $\{11\bar{2}1\}$ was found. In Fig. 5f, along with initially formed texture maxima, new maxima arose, conditioned by secondary twinning in grains with orientation *B* by planes $\{11\bar{2}1\}$. Twinning by these planes also continued up to the exhaustion of grains with an orientation corresponding to texture T1. The possibility of twinning explains the transition of texture T1 into texture T2, which consisted of a shift in texture maxima from the diameter ND-RD of stereographic projection to their final stable position at the diameter ND-TD. Thus, along with pyramidal, basal and prismatic slip caused by deformation degrees exceeding 50%, twinning by planes $\{11\bar{2}1\}$ also proved to be active in α-Zr. This fact did not agree with the conclusions of [14] concerning the suppression of twinning through the increase of deformation degree due to distortion of the deformed crystalline lattice.

Thus, up to ε=30% texture formation under rolling was provided by the active operation of twinning by planes $\{10\bar{1}2\}$, $\{10\bar{1}1\}$, $\{11\bar{2}1\}$ and $\{11\bar{2}2\}$. When the deformation degree exceeded 30%, twinning by planes $\{11\bar{2}1\}$ remained the active plastic deformation mechanism.

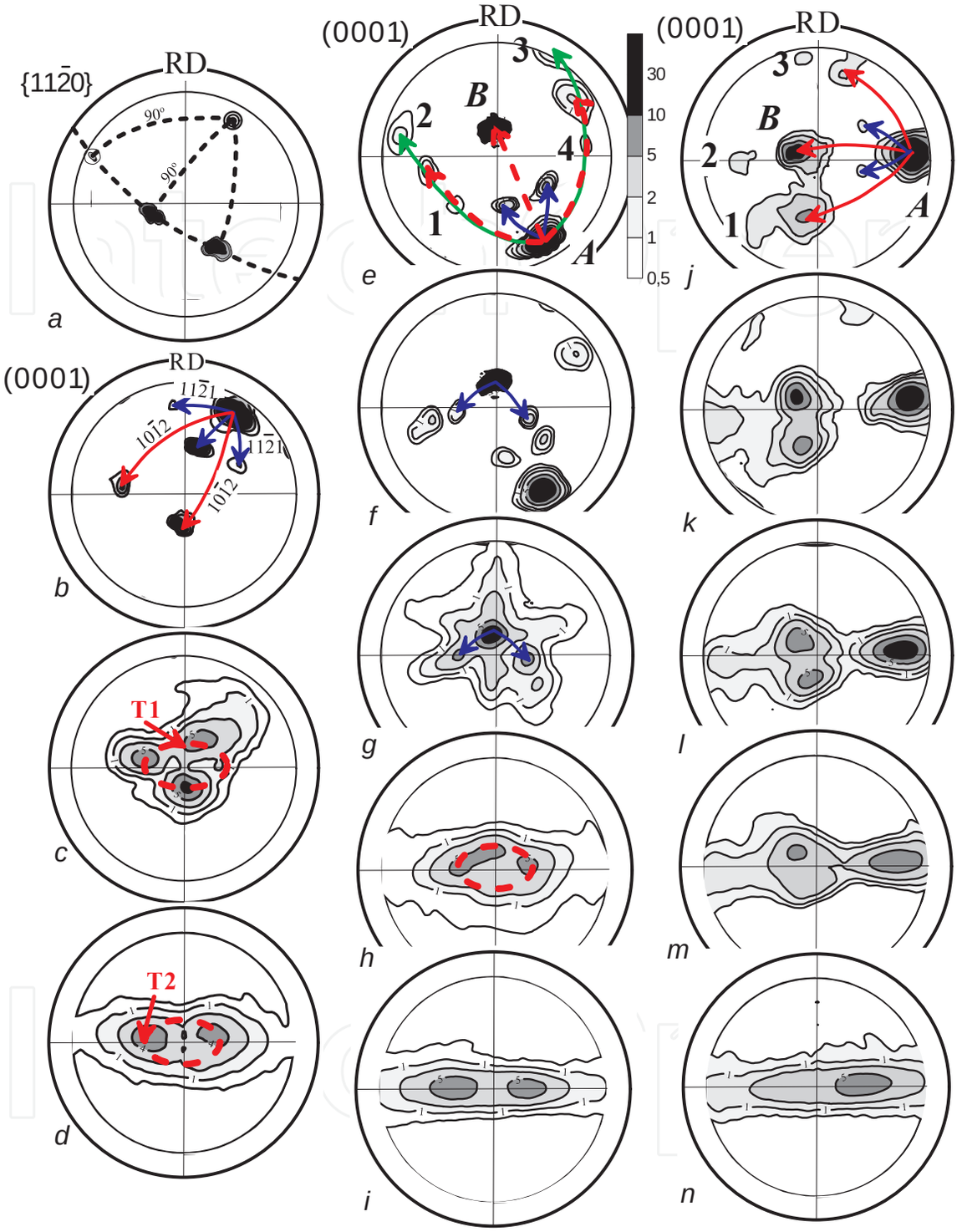

Single crystal N1:*b)*ε≈5 %;*c)*ε≈53 %;*d)* –ε≈80 %;
Single crystal N2: *e)*ε≈5 %;*f)*ε≈13 %; *g)*ε≈51 %; *h)*ε≈71 %; *i)*ε≈90 %;
Single crystal N3:*j)*ε≈7 %;*k)*ε≈30 %; *l)*ε≈50 %; *m)*ε≈70 %;*n)*ε≈98 %

Figure 5. PF{11$\bar{2}$0} of initial zirconium single crystal (a) and changes of PF (0001)due to twinning upon the rolling of α-Zr single crystals with different orientations:

4.2. Texture changes by slip

Fig. 5b and c, and Fig. 6c show that twinned areas of single crystals (fragments separated from other parts of a single crystal by planes of twinning) shift gradually to the centre of PF(0001), i.e., to ND of the rolled plate. Such a shift of texture maxima is conditioned by the development of a basal slip in the material. Along with clearly expressed additional texture maxima arising (see Fig. 5j), situated at the diameter ND-TD and symmetrically relative to ND, and connected with twinning by planes {11$\bar{2}$1}, formation of the elliptical texture maxima around ND can be observed. This maximum is markedby the dotted line in Fig. 5c and h, and serves as a boundary between regions of stereographic projection, with predominant activation of the pyramidal and basal slip systems [5], which provides the stability of the observed texture by intermediate deformation degrees of 50-70%. Observed gradual changes of the texture maximum position in Fig. 5k-n and Fig. 6c can be connected only with operation of the basal slip or through twinning by planes {11$\bar{2}$1}, resulting in the asymmetry of PF(0001) for rolled single crystal N 3, even at a deformation degree of 98%.

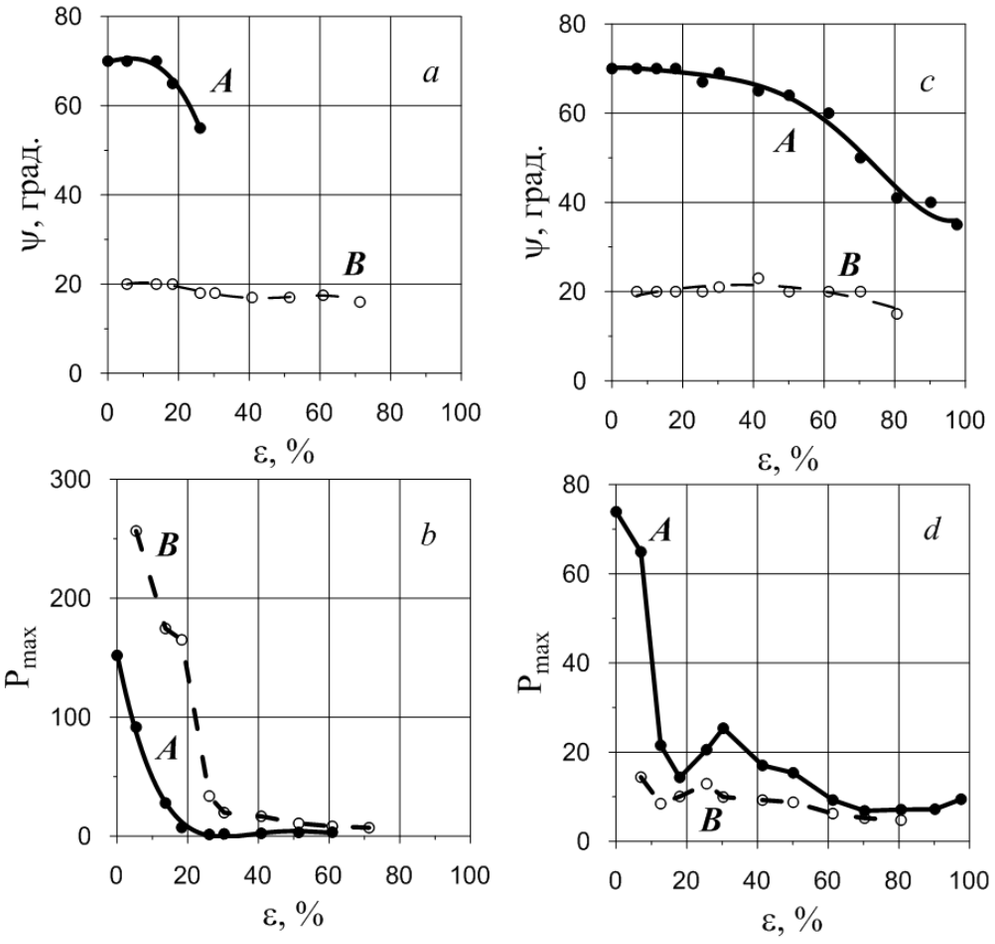

Figure 6. Changes in the pole coordinate ψ (a, c) and intensity (b, d) of texture maxima *A* and *B* (see Figure 5i, j) by increasing the deformation degree of *α*-Zr single crystals N 2 (a, b) and N 3 (c, d).

4.3. Recrystallization of rolled α-Zr single crystals

Results of the X-ray study of recrystallization in rolled α-Zr single crystals are presented in Fig. 7 and 8 for single crystal N 1, in Fig. 9 and 10 for single crystal N 2 and in Fig. 11 and 12 for single crystal N 3. The texture PF(0001) for rolled samples and recrystallized samples are shown in these figures as (*a*) and (*b*), respectively. For single crystals N 1 rolled at 53% and 80%, GPF β_{0002} were measured (Figs. 7c and 8c). For all rolled and recrystallized single crystals, subtraction diagrams $S(\psi, \varphi) = [PF(0001)_{recr} - PF(0001)_{roll}]$ are shown as (*d*). In Figs. 7e and 8e, diagrams of correlation between PF(0001) and GPF β_{0002} are presented. Each point in the diagrams corresponds to points with coordinates (ψ, φ) in PF and GPF at that values of pole density $P(\psi, \varphi)$, and are indicated in the axis of abscissas, whereas values of X-ray line half-width β_{0002} are showing the axis of ordinates.

The X-ray method of GPF, used for rolled single crystals in the current case characterized the condition of the crystalline lattice along basal axes <0001> in all fragments of the sample. As a measure of lattice distortion, which strengthens as a result of strain hardening and is removed by recrystallization, the physical angular half-width of the X-ray line (0002) β_{0002} was applied. A wide spectrum of substructure conditions, i.e., values of β_{0002}, responded to separate fragments of the rolled single crystal. In subtraction diagrams $S(\psi, \varphi) = [PF(0001)_{recr} - PF(0001)_{roll}]$ for each point (ψ, φ) of the stereographic projection, the difference between the pole densities of recrystallized and a rolled single crystal was calculated. The presented subtraction diagrams visually demonstrated the arrangements of regions where maximal changes of pole density by recrystallization were observed. Gradations of red colour in the subtraction diagram indicate regions of positive values and respond to an increase in pole density as a result of recrystallization, whereas gradations in blue colour correspond to a decrease of pole density due to recrystallization. Diagrams of correlation between PF(0001) and GPF β_{0002}, shown in Figs. 7e and 8e, had an appearance typical to that of a first approximation for many deformed metal materials, characterized by a gradual decrease of values β_{0002} as the peak of the texture maximum approached. Against a background of this tendency features can be observed as clearly connected to the character of corresponding rolling textures.

Due to the use of rolled α-Zr single crystals, the rolling textures obtained were formed mainly by twinning. In particular, in a single crystal N 1 rolled at 53%, i.e., by means of twinning, the rolling texture arose with maxima, which in spite of a relatively high deformation degree, took up transition positions, distinguishing them from maxima in stable textures T1 and T2. Subtraction diagrams showed that in the case of recrystallization within regions of PF for a rolled single crystal, where texture maxima arose due to twinning, the growth of pole density was absent (Fig. 7a, d). In fragments of rolled single crystals corresponding to the orientation of their basal axes near normal direction ND, rolling can activate only a pyramidal slip, characterized by high values of critical shear stress. Operation of other slip systems in these fragments (or grains of polycrystal) is suppressed due to low Schmidt factor values. Therefore, in fragments of α-Zr single crystals (or the grains of a polycrystal) experiencing reorientation, predominantly through the participation of twinning, their strain hardening, including distortion of the crystalline lattice and fragmentation of substructure elements, is relatively small. So, during the course of subsequent annealing, nuclei of recrystallization do not arise in these regions and these fragments (or grains of polycrystal) are swallowed up by recrystal-

http://dx.doi.org/10.5772/60019

lization nuclei, growing more actively and corresponding by their orientation to regions of PF with increased strain hardening. GPF β_{0002} for rolled single crystals N 1 in Figs. 7c and 8c also indicate that the strain hardening of fragments with a basal axis orientation near ND is minimal. For this reason, in subtraction diagrams constructed for all rolled single crystals, we see a blue centre, testifying that in the central region the growth of pole density by recrystallization was absent, since the only mechanism provided here in terms of its input was twinning.

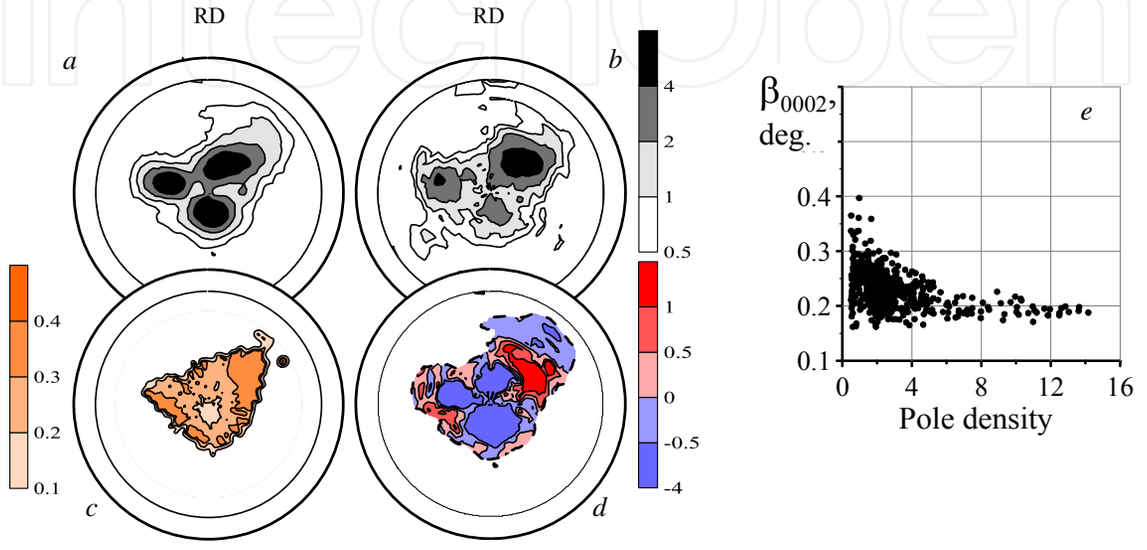

Figure 7. Recrystallization in cold-rolled α-Zr single crystal N 1 (ε~50%): *a* – PF(0001)$_{roll}$, *b* - PF(0001)$_{recr}$; *c* – GPF β_{0002}; *d* – [PF(0001)$_{recr}$- PF(0001)$_{roll}$]; *e* – diagram of correlations between PF(0001) and GPFβ_{0002}.

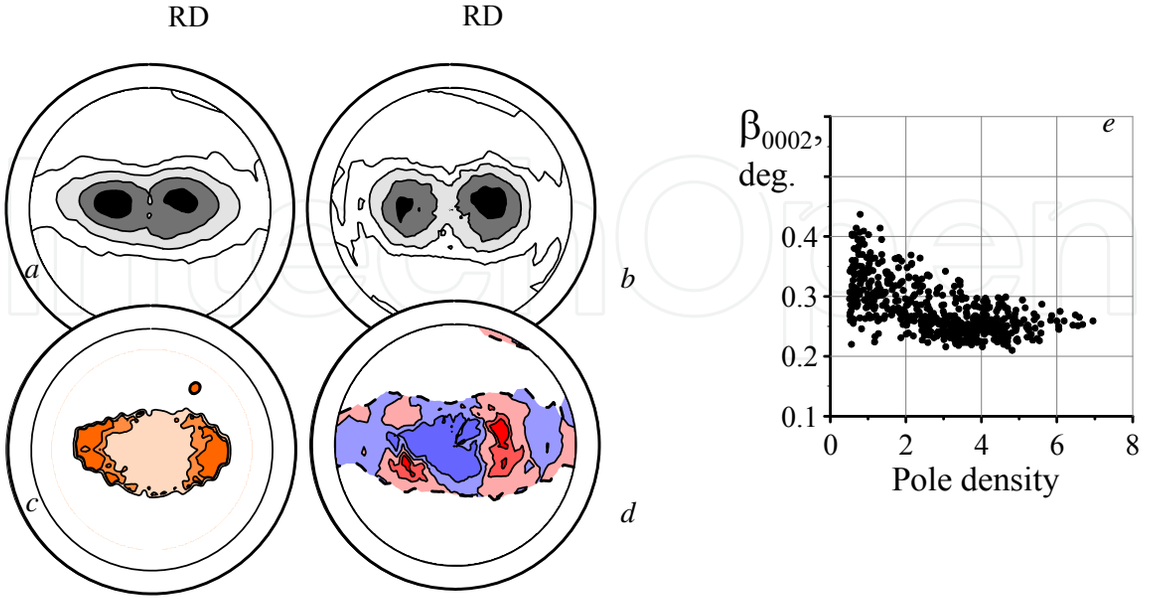

Figure 8. Recrystallization in cold-rolled α-Zr single crystal N 1 (ε~80%): *a* – PF(0001)$_{roll}$, *b* - PF(0001)$_{recr}$; *c* – GPF β_{0002}; *d* – [PF(0001)$_{recr}$- PF(0001)$_{roll}$]; *e* – diagram of correlation between PF(0001) and GPFβ_{0002}.

At the same time, the subtraction diagrams constructed for rolled single crystals show that its texture maxima are bordered by zones of intensive recrystallization (Fig. 7d). Only within these regions of stereographic projection was the increased lattice distortion also observed (Fig. 7c) as a consequence of the above-described simultaneous operation of the pyramidal and basal slip. According to GPF β_{0002}, the "slopes" of texture maxima (see Fig. 7c) respond to regions of greatest fragmentation and the distortion of the crystalline structure, so that in the current case, the main mechanism of α-Zr recrystallization was the intensive growth of regions in the deformed crystalline matrix with the increased energy of residual distortions.

As the deformation degree of single crystals increased, their rolling texture changed and acquired features of the texture T2 (Fig. 7-12). This testified that the relative input of twinning in the formation of new maxima gradually decreased and was replaced by the slip. When this happened, the character of subtraction diagrams and diagrams of correlation PF(0001) – GPF β_{0002} sharply changed. In the subtraction diagrams, additional red regions arose, coinciding approximately with the positions of T2 maxima in rolling textures. Hence, the strain hardening at these maxima was higher than in regions where twinning had previously been predominant and here, a greater number of recrystallization nuclei arose (Fig. 8, 10, 12).

The most detailed and precise data concerning the evolution of strain hardening distributions in rolled single crystals provided diagrams of correlation PF(0001) – GPF β_{0002}, showing in Figs. 7e and 8e. Texture maxima, formed by twinning, were twice as high as those formed by the slip at a later stage. Strain hardening of fragments corresponding to these maxima by ε=53% was constant and remained low (β_{0002}< 0,2°) for the most part, whereas for ε=80% strain hardening as noticeably higher (β_{0002}> 0,25°) and varied within significant intervals. The correlation diagrams show that strain hardening grew as an angular distance of the considered fragment from the top of maxima increases. The reason for this regularity was the different features of the slip within the stable texture maxima and at their periphery parts, i.e. at texture minima, where pole density is lower than 1. Stable texture maxima arose in regions of stereographic projection, where the operation of different slip systems was equilibrated. In the case of α-Zr rolling stability of T2, texture maxima were conditioned through the mutually balanced operation of basal and prismatic slip systems. However, the joint activity of these slip systems resulted in increased strain hardening, whereas their alternating operation, realized in turn, that is one after another, led to a drop in strain hardening and was equivalent to the effect of the monoslip. The metal matrix adopted to the last variant of texture development as a means for requiring minimal energy expenditure; this variant of deformation development explained details concerning strain hardening and resulting recrystallization in the considered samples.

The opinion is widespread in literature that by recrystallization of α-Zr, the main mode of texture changes consists of the rotation of the lattice by 30° about the basal axis [13, 15]. Some studies, however, do not support this opinion [16-18]. In the current chapter, an attempt was made to explain the discrepancies in experimental data concerning this question. In Fig. 13 PF{11$\bar{2}$0}, rolled and recrystallized α-Zr single crystals are shown at the highest deformation degrees. Though the deformation degrees of rolled single crystals were high and the stable

http://dx.doi.org/10.5772/60019

distribution of basal axes already had time to form, the usual distribution of prismatic axes, characterized by regular arrangement of alternating in 60° maxima along the meridians of stereographic projection, almost did not develop. Since basal maxima are situated close to the centre of pole figure, prismatic axes are situated at the periphery of stereographic projection and are seen only partially. Smaller deformation degrees PF{11$\bar{2}$0} for rolled single crystals N1 and N 2 proved to be chaotic, so that the joint rotation by 30° of prismatic axes about the basal axis as a result of recrystallization could not be fixed.

This rotation means that in the rolled matrix there are recrystallization nuclei situated at the boundary between two deformed grains with close orientations, have a middle orientation and swallow grains of the matrix due to growing into these neighboring grains at equal rates. This mechanism can work only when the rolled matrix has developed a deformation texture, so that the rotation of prismatic axes by 30° is not the only possible situation in some fragments of the sample; instead, a more complex process takes place in a coordinated manner within the entire matrix. The misorientation of some newly originated nuclei by 30° with the deformed matrix can promote its growth, but it does not create the recrystallization texture in the absence of the developed rolling texture.

As for the rolled single crystal N 3 (Fig. 13e, f), this case deserves separate consideration. Due to the position of its basal axis near TD (Fig. 5j), the largest part of this single crystal deforms at first by means of a prismatic slip and only by $\varepsilon \approx 7\%$ the twinning is noticeable, overthrowing a portion of basal axes at the central segment of diameter ND-RD (Fig. 5m). PF{11$\bar{2}$0} of this single crystal after rolling (Fig. 13e) contains two branches: the left corresponds to the fraction deformed by the prismatic slip, i.e., to the developed rolling texture; the right corresponds to the twinned fraction, which is characterized by low strain hardening and a small number of recrystallization nuclei. Maxima in the right branch shifted up and down in correspondence to the position of twinned basal maxima near ND. The important feature of the rolled single crystal, as well as the rolled fine-grained polycrystal (revealed by their X-ray texture study) was the micro-scale of inhomogeneities, consisting in the approximate identity of results, which had been obtained through measurements of neighbouring regions. This result indicated that any region of the studied sample contained a statistically significant number of micro-fragments or grains with various orientations. As applied to the rolled single crystal N 3, this means, that its micro-fragment corresponded to both branches in PF{11$\bar{2}$0} (Fig. 13e), i.e., those deformed by prismatic slip, as well as small twins that can be their nearest neighbours in the microstructure of the sample. Therefore, as a result of recrystallization of this single crystal (Fig. 13f), the right twinned branch in PF{11$\bar{2}$0}, characterized by low strain hardening, proved to have been swallowed by nuclei from the left branch with the developed rolling texture. However, micro-fragments deformed by the prismatic slip after recrystallization did not indicate a clear rotation by 30°, since among the nearest neighbours of these micro-fragments small twins were present and the deformed matrix had been broken into particles with alternating characteristics, and coordinated rotation of this matrix proved to be impossible. Nevertheless, a number of weak signs of such future rotation were seen within the left branch of the pole density distribution in Fig. 13f.

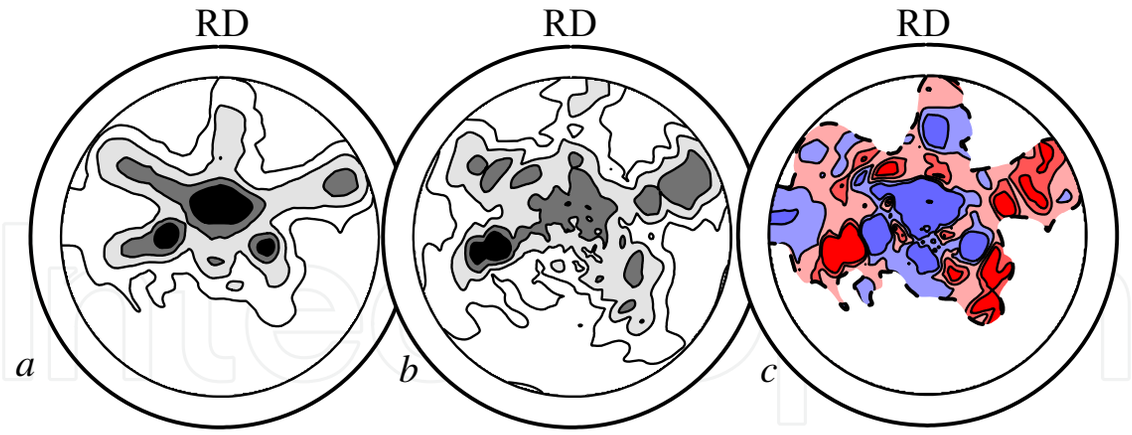

Figure 9. Recrystallization in cold rolled α–Zr single crystals N 2 (ε~30%): *a* – $PF(0001)_{roll}$, *b* - $PF(0001)_{recr}$; *c* – [$PF(0001)_{recr}$- $PF(0001)_{roll}$].

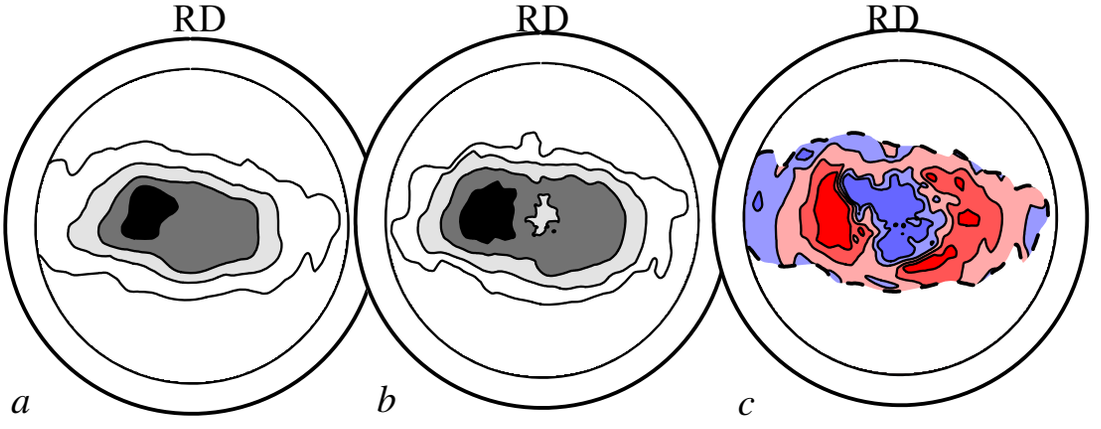

Figure 10. Recrystallization in cold rolled α–Zr single crystals N 2 (ε~70%) : *a* – $PF(0001)_{roll}$, *b* - $PF(0001)_{recr}$; *c* – [$PF(0001)_{recr}$- $PF(0001)_{roll}$].

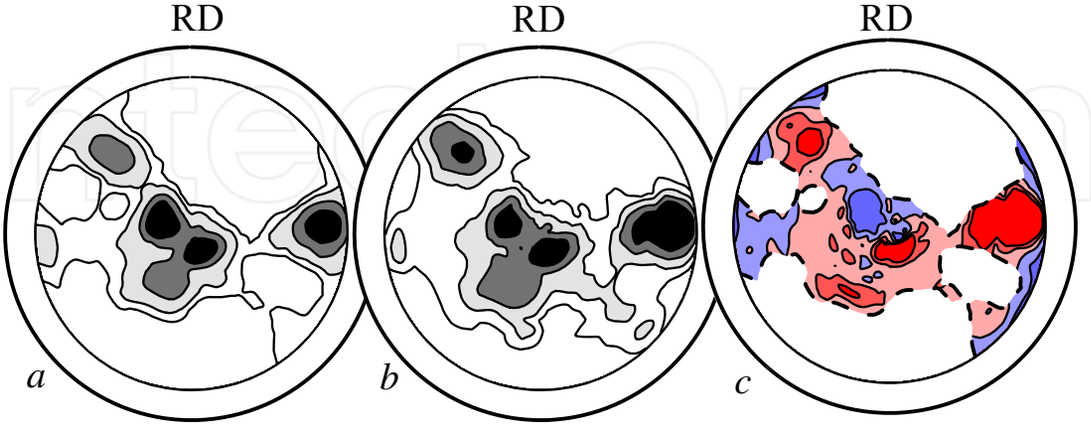

Figure 11. Recrystallization in cold rolled α–Zr single crystals N 3 (ε~30% (*a-c*) and ε~70% (*d-f*)): *a* – $PF(0001)_{roll}$, *b* – $PF(0001)_{recr}$; *c* – [$PF(0001)_{recr}$- $PF(0001)_{roll}$].

http://dx.doi.org/10.5772/60019

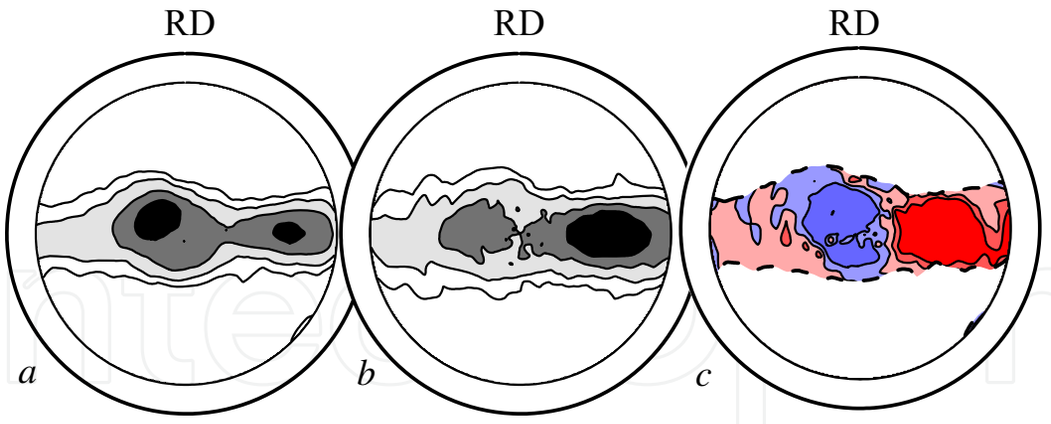

Figure 12. Recrystallization in cold rolled α–Zr single crystals N 3 (ε~30% (*a-c*) and ε~70% (*d-f*)): *a*– PF$(0001)_{roll}$, *b* – PF$(0001)_{recr}$; *c* – [PF$(0001)_{recr}$- PF$(0001)_{roll}$].

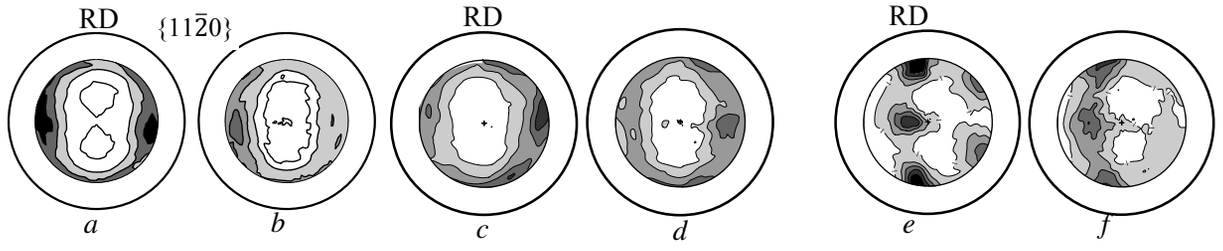

Figure 13. Texture changes through the recrystallization of rolled α-Zr single crystals N 1, ε=80% (*a, b*), N 2, ε=70% (*c, d*) and N 3, ε= 70% (*e, f*). (*a, c, e*): PF {11$\bar{2}$0} for rolled single crystals; (*b, d, f*):PF {11$\bar{2}$0} for rolled and annealed single crystals 580°C/3 h.

4.4. Recrystallization of polycrystalline α-Zr sheets in light of data, obtained for recrystallization of rolled α-Zr single crystals

The consideration of data regarding the recrystallization of a rolled α-Zr single crystal can be used for explaining the features of polycrystalline α-Zr sheets observed during their recrystallization. In Figs. 14 and 15, the results of X-ray diffractometric studies of iodide coarse-grained α-Zr rolled, respectively, by 50% and 70% and then recrystallized, are presented. In Figs. 16 and 17, analogous data are presented for α-Zr in a polycrystalline Zr-1%Nb alloy, rolled by 70% along and across the initial RD, respectively, and finally, recrystallized. In all Figures PF(0001), rolled samples are shown as (a), PF(0001) for recrystallized samples – as (b); GPF_{0002}– as (c); subtraction diagrams S(ψ, φ) - as (d) and diagrams of correlation PF(0001) - GPF β_{0002}- as (e). In Fig. 18, polycrystalline materials PF{11$\bar{2}$0} are shown for both rolled and recrystallized conditions.

According to models of texture formation in α-Zr [13, 19], the pole density in the central region of PF(0001) is conditioned by the input of grains experiencing twinning by deformation.

Subtraction diagrams show that under recrystallization in the corresponding regions of PF for the deformed samples, an increase of pole density was absent. The reasons for this effect in polycrystalline α-Zr sheets are the same as for rolled single crystals. The absence of growth of α-Zr grains with orientations corresponding to the central region of PF(0001) has been noted in previous studies dealing with the recrystallization of products from Zr-based alloys [8, 20]. However, only experiments with the rolling and recrystallization of α-Zr single crystals have yielded a direct demonstration of the effect as influenced by twinning on the strain hardening and the subsequent recrystallization of α-Zr crystallites.

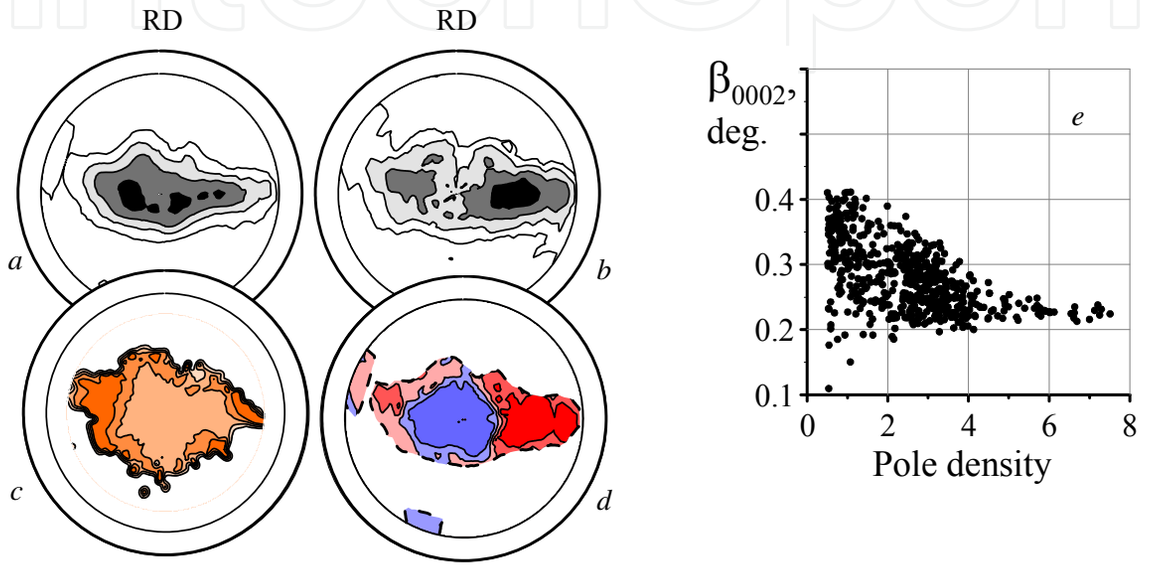

Figure 14. Recrystallization of polycrystalline rolled iodide α-Zr (ε~50%): *a* – PF$(0001)_{roll}$, *b* - PF$(0001)_{recr}$; *c* – GPF β_{0002}; *d* – [PF$(0001)_{recr}$- PF$(0001)_{roll}$]; *e* - diagram of correlation PF(0001) - GPF β_{0002}.

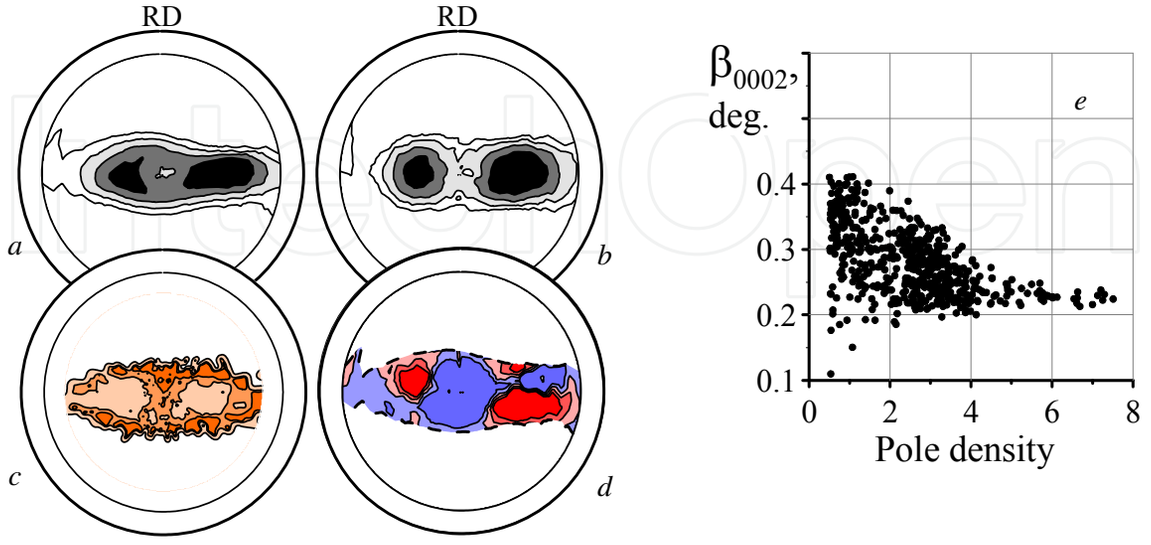

Figure 15. Recrystallization of polycrystalline rolled iodide α-Zr (ε~80%): *a* – PF$(0001)_{roll}$, *b* - PF$(0001)_{recr}$; *c* – GPF β_{0002}; *d* – [PF$(0001)_{recr}$- PF$(0001)_{roll}$]; *e* - diagram of correlation PF(0001) - GPF β_{0002}.

http://dx.doi.org/10.5772/60019

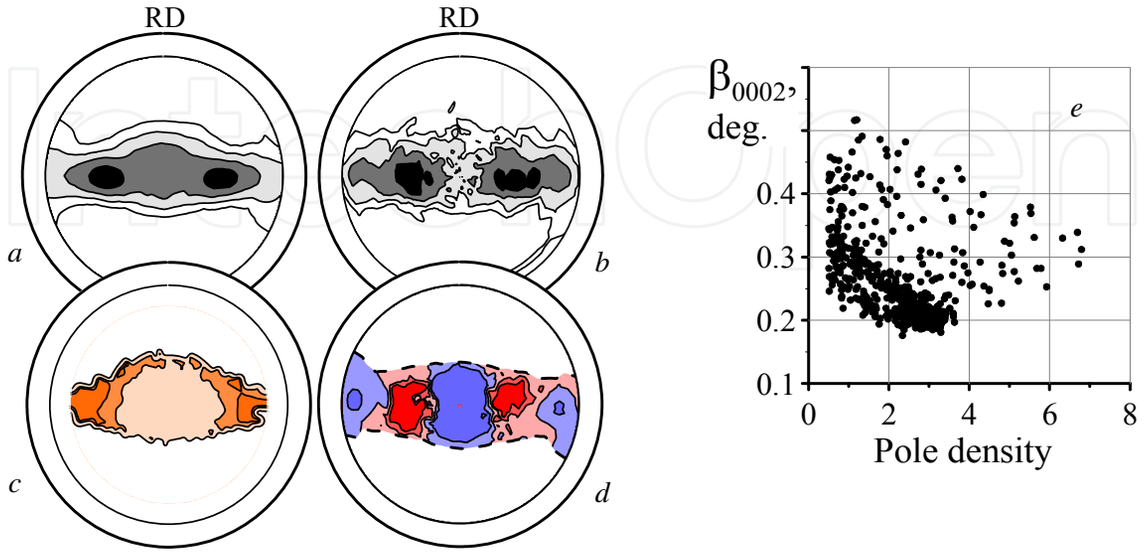

Figure 16. Recrystallization of Zr-1%Nb alloy rolled along initial RD (ε~50%): *a* – PF(0001)$_{roll}$, *b* - PF(0001)$_{recr}$; *c* – GPF β_{0002}; *d* – [PF(0001)$_{recr}$- PF(0001)$_{roll}$]; *e* - diagram of correlation PF(0001) - GPF β_{0002}

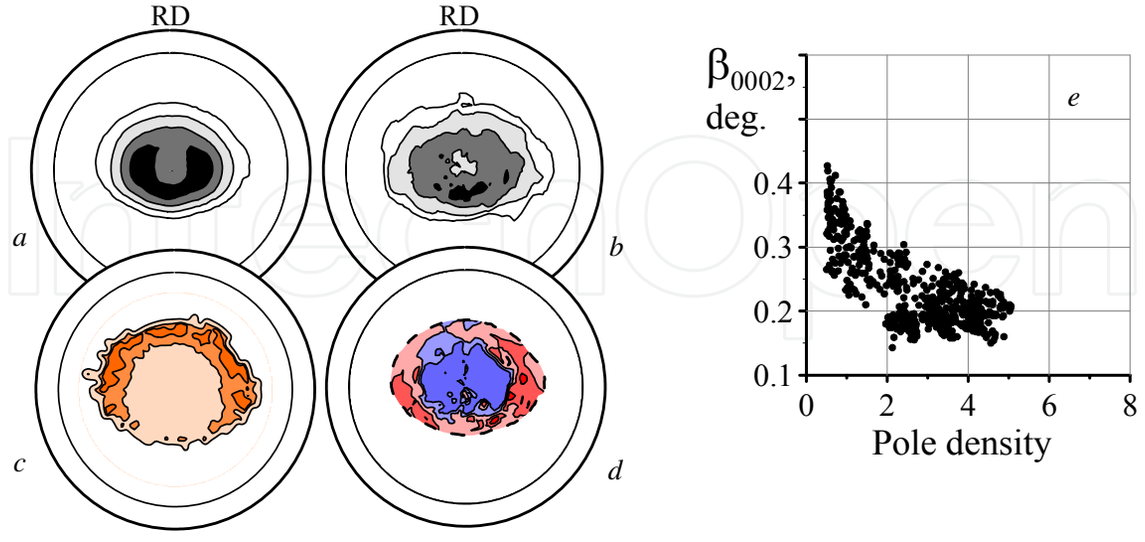

Figure 17. Recrystallization of Zr-1%Nb alloy rolled across initial RD (ε~50%): *a* – PF(0001)$_{roll}$, *b* - PF(0001)$_{recr}$; *c* – GPF β_{0002}; *d* – [PF(0001)$_{recr}$- PF(0001)$_{roll}$]; *e* - diagram of correlation PF(0001) - GPF β_{0002}

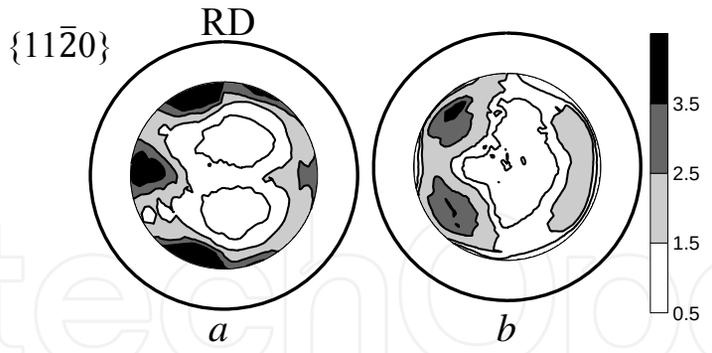

Figure 18. Texture changes through recrystallization of rolled Zr single crystals N 1 (a, b), N 2 (*c*, *d*) and N 3 (e, f). (a, c, e) DPF {11$\bar{2}$0} for rolled single crystals with deformation degrees: ε=80, 70 and 70%, respectively; (b, d, f) annealing 580°C – 3 h.

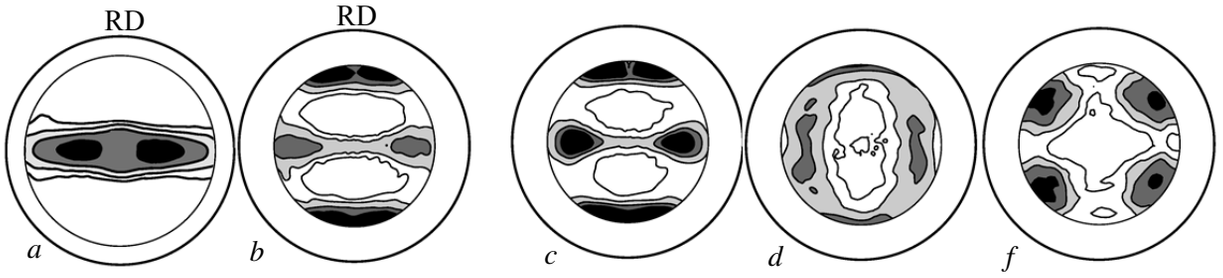

Figure 19. PF (0001) (a) and PF{11$\bar{2}$0} (b) for the rolled Zr–1% Nb plate; changes in PF{11$\bar{2}$0} due to recrystallization annealing upon heating at different rates: (c) 100, (d) 20, and (e) 2°/min.

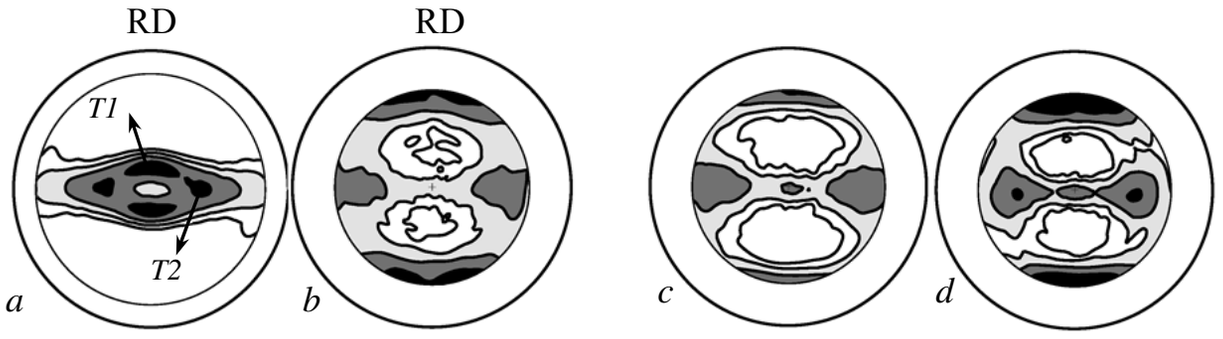

Figure 20. PFs (0001) (a) and {11$\bar{2}$0} (b) of the rolled Zr–1% Nb plate with texture components T1 and T2 in the initial state and changes in PF{11$\bar{2}$0} due to recrystallization annealing upon heating at different rates: (c) 100 and (d) 2°/min.

Shifts in the maxima rolling textures of polycrystalline Zr sheets by recrystallization are explained by the preferential growth of grains with basal axes orientations at the outward edges of these maxima. Here, there are more recrystallization nuclei and new grains that arise here absorb deformed grains localized within previous maxima textures (Fig. 14-17d). This shift occurs due to the inhomogeneity of strain hardening in the rolled samples, consisting first

http://dx.doi.org/10.5772/60019

of all in its strengthening with increase of an angular distance of crystallite from texture maximum. This effect is clearly seen in Figs. 14-17 and has the same nature as bordering maxima textures with zones of increased strain hardening and intensive growth of recrystallized grains in rolled single crystals. The outward edge of different stable texture maximum slip systems, i.e., basal and prismatic systems, act together and since the volume of material to be deformed here is relatively small, simultaneous operation of both systems is possible. However, when moving inside the stable texture maximum, these slip systems begin to operate alternately in each point of the sample. As a result of recrystallization, new maxima grows at "slopes" of initial maxima in the rolling texture. Here, the strain hardening is sufficiently high for providing the preferential growth of arising nuclei, while at the same time the number of grains located at this segment of "slope" is sufficiently large for absorbing the entire deformed matrix. Obviously, this feature is typical for all metal material at the deformation stage and corresponds to the maxima arising in their deformation textures. Features of their recrystallization at the first approximation reflect the characteristics of strain hardening distribution, formed during the course of their rolling.

In terms of data related to the sample of Zr-1%Nb alloy rolled across initial RD, we observed that this sheet was characterized by the same features of strain hardening distribution and recrystallization development, the only difference being the space isotropy of constructed diagrams. As a result of symmetry, the obtained data were confirmed to be statistically safer.

In rolled Zr single crystal, deformed up to 80% by means of twinning and predominantly consisting of basal and pyramidal slips (Fig. 5b), after annealing at 580°C, a noticeable rotation of prismatic axes was not observed (Fig. 13). At the same time, in polycrystalline Zr rolled up to 80% (Fig. 15), after recrystallization, the sharp reorientation of prismatic axes became apparent (Fig. 18) by means of their rotation at 30° about the basal axis, coinciding with the correct texture maximum (Fig. 15b). It was evident that the rotation of prismatic axes about basal axes took place only in cases when recrystallized areas of α-Zr were deformed by rolling and with the inclusion of a prismatic slip, which according to Hobson's scheme [2], develops within wide regions of stereographic projection adjacent to TD. The development of stable α-Zr rolling texture is always realized by active participation of a prismatic slip, since the existence of texture maxima at a horizontal diameter of PF(0001) is conditioned by the mutually balanced operation of a slip in the prismatic and basal planes [6]. Only in a case where texture maxima are distanced from ND by a comparatively small angular distance, as in PF(0001) of the single crystal rolled to ~50%, can one certify that a prismatic slip did not participate in the formation of texture.

Increasing the heating rate up to attainment of the recrystallization temperature (see Fig. 19c, d and f) or the presence of additional components in the texture of the rolled sheet, for example, T1+T2 (Fig. 20), prevents the rotation of prismatic axes.

Analysis of data regarding the rotation of prismatic axes under annealing of rolled α-Zr allows for ascertaining the mechanism of its recrystallization, established earlier by considering strain hardening distributions using GPF β_{0002}. The presented data testify that in α-Zr by recrystallization, the mechanism is realized by combining two different aspects:

1. the rotation of basal axes in accordance with the strain hardening distribution, revealed with the help of GPF β_{0002} and predetermining the predominant growth of regions responding by their orientation to "slopes" of maxima in the rolling texture;
2. the nuclei of recrystallization formed in these regions during the course of their growth can cause (or not) 30° rotation of the matrix, depending on the participation of the prismatic slip in their deformation.

From nuclei arising in zones of increased strain hardening and having all possible orientations, the matrix chooses nuclei characterized by a 30°angle of misorientation at the boundaries as the best prospects for future growth. The increased heating rate by annealing of material and the presence in the deformed matrix of layers of grains with other orientations [8, 9] prevent such selection (Figs. 13, 20).

Dependence of the observed reorientation of prismatic axes on the heating rate of the sample can be explained in the following manner: the growth of recrystallization nuclei as part of the diffusion process requires a definite time period for the revealing of these nuclei, which are capable of swallowing the deformed matrix and to impose its own orientation as a result of the optimal angle of misorientation at grain boundaries.The presence in the deformed matrix of layers of grains with orientations of RD different from $\{10\bar{1}0\}$ also prevents rotation of the matrix by 30°, as does the violation of the optimal 30° misorientation at all boundaries of growing nuclei and grains of matrix [15].

5. Conclusions

1. Experiments with rolling and annealing of α-Zr single crystals helped to understand the mechanisms of α-Zr recrystallization in polycrystalline products, the absence of grain growth in regions of predominant twinning, rotation of the deformed α-Zr matrix about the basal axis and the conditions for the preferential growth of new grains.
2. Regions of the α-Zr matrix deformed by predominant participation of twinning were characterized by minimal strain hardening, by an insignificant number of recrystallization nuclei and a decreased trend towards grain growth, so that under recrystallization, these regions were swallowed by those that had higher strain hardening.
3. The necessary condition for 30° rotation of the deformed matrix about the basal axis through recrystallization of rolled α-Zr consisted predominantly of the participation of a prismatic slip in its plastic deformation.
4. In the course of α-Zr recrystallization the following mechanism for the preferential growth of definite regions was realized: these regions were characterized by relatively high strain hardening and orientations "slopes" of maxima in the rolling texture, where number of grains was sufficiently great in order to swallow the whole α-Zr matrix. Deformation of the α-Zr matrix at these "slopes" was realized by the simultaneous joint operation of basal, prismatic and pyramidal slip systems, whereas in central regions of maxima these systems operated alternately and provided minimal strain hardening.

5. By the quick heating of rolled samples with the purpose of their recrystallization, rotation of the deformed matrix by 30° about its basal axis did not take place, as in the case, when additional components were present in the rolling texture.

Author details

Yu Perlovich* and M. Isaenkova

*Address all correspondence to: yuperl@mail.ru

Department of Materials Science, National Research Nuclear University MEPHI (Moscow Engineering Physics Institute), Kashirskoe shosse, Moscow, Russia

References

[1] Perlovich Yu., Bunge H.J., Isaenkova M. Structure inhomogeneity of rolled textured niobium. Zeitschrifft fur Metallkunde, Materials Research and Advanced Techniques 2000; 91(2) 149-159.

[2] Hobson D.O. Textures in Deformed Zirconium Single Crystals. Transactions of Metallurgical Society AIME 1968;242 1105-1110.

[3] Perlovich Yu.A., Isaenkova M.G. Reorientation of α-Zr Crystallites under Rolling. Russian Metallurgy (Metalli) 1987;3 152-155.

[4] Isaenkova M.G., Perlovich Yu.A. Role of Twinning in Development of Deformation Texture in α-Zr. Physics of Metals and Metallography 1991;5 87-92.

[5] Matcegorin I.V., Rusakov A.A., Evstyukhin A.I. Analysis of Mechanism of Texture Formation in α-Zr by Use of IBM Modelling. In book: Metallurgy and Materials Science of Pure metals. Moscow: Atomizdat 1980;14 39-52.

[6] Isaenkova M. G. and Perlovich Yu. A. Kinetics and Mechanisms of Texture Formation in α-Zirconium upon Rolling. Physics of Metals and Metallography 1987; 107-112.

[7] Tenckhoff E. The Development of the Deformation Texture in Zirconium during Rolling in Sequential Passes. Met. Transactions A 1978;9 1401-1412.

[8] Perlovich Yu., Isaenkova M. Regularities of Recrystallization in Sheets and Tubes of Zr-Alloys. // Microstructural and Crystallographic Aspects of Recrystallization, Roskilde, Denmark, 1995, p. 371-376.

[9] Perlovich Yu., Isaenkova M. Recrystallization. Ed. K. Sztwiertnia, InTech, Croatia. p. 1-20.

[10] Perlovich Yu. Development of Strain Hardening Inhomogeneity during Texture Formation under Rolling of bcc Metals. In: Numerical Prediction of Deformation Processes and the Behaviour of Real Materials. Proceedings of the 15thRiso International Symposium on Materials Science. Ed. by S.Y. Andersen et al., Riso National laboratory, Roskilde, Denmark, 1994, p. 445-450.

[11] Perlovich Y., Isaenkova M., Bunge H.J. General Newly-Discovered Regularities of Structure Inhomogeneity in Textured Metal Materials. Materials Science Forum 2001;378-381 174-179.

[12] Isaenkova M.G., Perlovich Yu.A., Fesenko V.A. Modern Methods to Construct Experimentally Texture Complete Direct Polefigures by X-ray Data. Industrial Laboratory. Materials Diagnostics 2013;79(7) 1 25-32.

[13] Kocks U.F., Tome C.N., Wenk H.R. Texture and Anisotropy. Preferred Orientation in Polycrystals and their Effect on Materials Properties. Cambridge University Press, 1998. 676 p.

[14] Phillippe M., Phillippe M.J. Texture Formation in Hexagonal Materials. In: Texture of Materials ICOTOM-10, H.J. Bunge, ed. (Switzerland, Trans. Tech. Publ.), 1994, p. 1337-1350.

[15] Recrystallization of Metallic Materials. Ed. By F. Haessner, Dr.Riederer Verlag GmbH, Stuttgart, 1978, s. 293.

[16] Dewobroto N., Bozzolo N., Batberis P., Wagner F. On the Mechanisms Governing the Texture and Microstructure Evolution during Static Recrystallization and Grain Growth of Low Alloyed Zirconium Sheets. International Journal of Material Research 2007;97 826-833.

[17] Wagner F., Bozzolo N., Van Landuyt O., Grosdidier T. Evolution of Recrystallization Texture and Microstructure in Low Alloyed Titanium Sheets. Acta Materialia 2002;50 1245-1259.

[18] Gerspach F., Bozzolo N., Wagner F. On the Stability of Recrystallization Texture in Low Alloyed Titanium Sheets. Application of Texture Analysis, Ceramic Transactions 2008;201 593-600.

[19] Tenckhoff E. Deformation Mechanisms, Texture and Anisotropy in Zirconium and Zircaloy. ASTM, Special Technical Publication (STP 966), Philadelphia, 1988. 77 p.

[20] M.G. Isaenkova, Yu.A. Perlovich, V.A. Fesenko, O.A. Krymskaya, N.A. Krapivka, Soe San Tkhu. Regularities of Recrystallization of Rolled Single Crystals and Polycrystals of Zirconium and Alloy Zr-1%Nb. The Physics of Metals and Metallography August 2014;115(8) 756-764.